CHAPTER I

1. INTRODUCTION

1.1. Quantum confinement effect-an overview

The most popular term in the nano world is *quantum confinement effect* which is essentially due to changes in the atomic structure as a result of direct influence of ultra-small length scale on the energy band structure (Takagahara and Takeda 1992a, Wise 2000, Zhao et al. 2004). The length scale corresponds to the regime of quantum confinement ranges from 1 to 25 nm for typical semiconductor groups of IV, III-V and II-VI. In which the spatial extent of the electronic wave function is comparable with the particle size. As a result of these "geometrical" constraints, electrons "feel" the presence of the particle boundaries and respond to changes in particle size by adjusting their energy. This phenomenon is known as the quantum-size effect. Quantization effects become most important when the particle dimension of a semiconductor near to and below the bulk semiconductor Bohr exciton radius which makes materials properties size dependent. In general, the Bohr radius of a particle is defined as (Yoffe 1993),

$$a_B = \varepsilon \frac{m}{m^*} a_o \qquad \text{----------------------} \quad (1)$$

where ε is the dielectric constant of the material, m* is the mass of the particle, m is the rest mass of the electron, and a_o is the Bohr radius of the hydrogen atom. When the particle size approaches Bohr exciton radius, the quantum confinement effect causes increasing of the excitonic transition energy and blue shift in the absorption and luminescence band gap energy (Yoffe 1993). For example, 4.8 nm diameter PbSe NCs show an effective band gap of approximately 0.82 eV, exhibiting a strong confinement induced blue shift of >500 meV compared to the bulk PbSe band gap of 0.28 eV (the Bohr exciton radius in PbSe is 46 nm) (Wise 2000). In addition, quantum confinement leads to a collapse of the continuous energy bands of a bulk material into discrete, atomic like energy levels. The discrete structure of

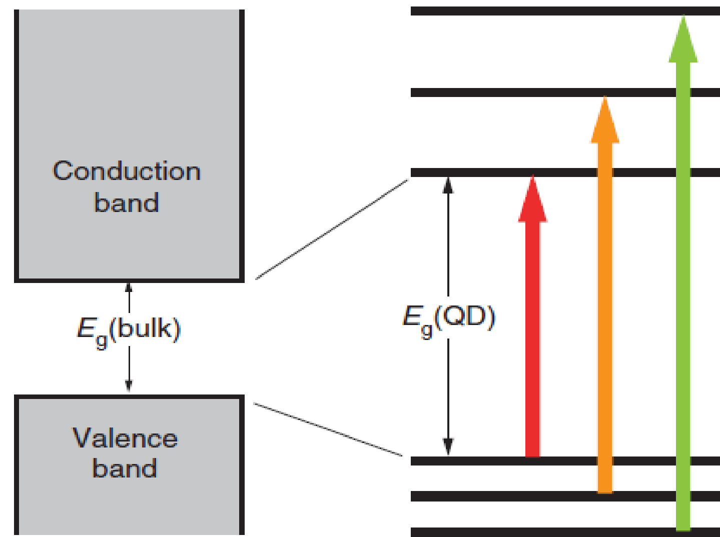

Fig. 1.1: *A schematic of the discrete energy level of a semiconductor.*

energy states leads to a discrete absorption spectrum, which is in contrast to the continuous absorption spectrum of a bulk semiconductor as shown in Fig. 1.1. A quantum confined structure is one in which the motion of the carriers (electron and hole) are confined in one or more directions by potential barriers (Miller et al. 1984). Based on the confinement direction, a quantum confined structure will be classified into three categories as quantum well, quantum wire and quantum dots or nanocrystals. The basic type of quantum confined structure is shown in Table 1.1.

Table 1.1: *Classification of quantum confined structures.*

Structure	Quantum confinement	Number of free dimension
Bulk	0	3
Quantum well/superlattices	1	2
Quantum wire	2	1
Quantum dot/Nanocrystals	3	0

In QDs, the charge carriers are confined in all three dimensions which the electrons exhibit a discrete atomic-like energy spectrum. Quantum wires are formed when two dimensions of the system are confined. In quantum well, charge carriers (electrons and holes) are confined to move in a plane and are free to move in a two-dimensional. Also the energy level of one of the quantum numbers changes from continuous to discrete. Compared with bulk semiconductors, the quantum well has a higher density of electronic states near the edges of the conduction and valence bands, and therefore a higher concentration of carriers can contribute to the band-edge emission (Chen et al. 2012). As more number of the dimension is confined, more discrete energy levels can be found, in other words, carrier movement is strongly confined in a given dimension. Density of electron states in bulk, 2D, 1D and 0D semiconductor structure is shown in Fig. 1.2. 0D structures has very well defined and quantized energy levels. The quantum confinement effect corresponding to the size of the nanostructure can be estimated via a simple effective-mass approximation model.

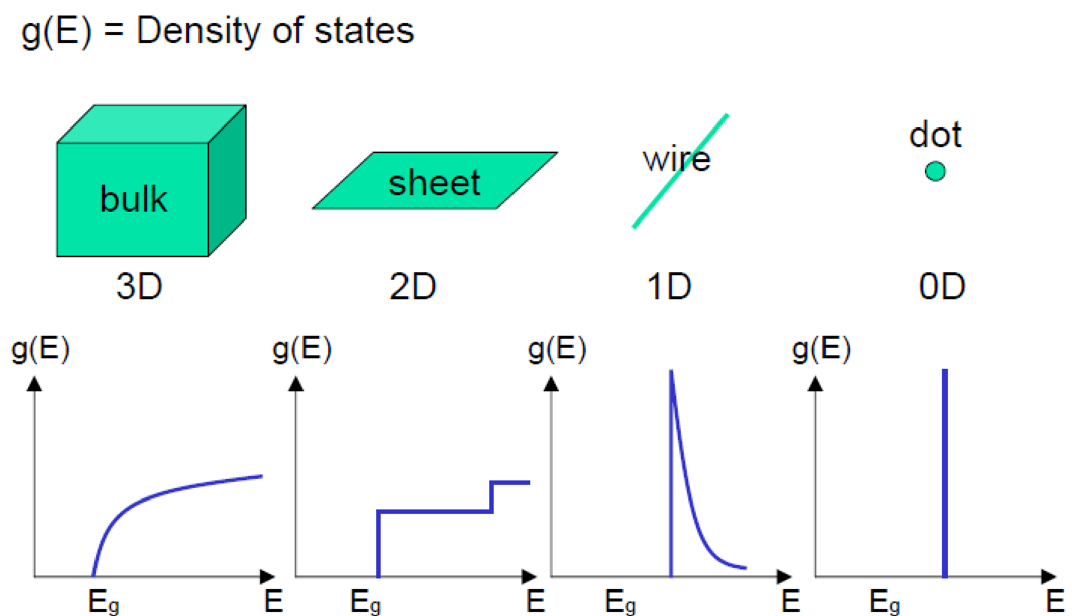

Fig. 1.2: *Density of electron states of a semiconductor as a function of dimension. The optical absorption spectrum is roughly proportional to the density of states.*

This method can predict the confined energy levels of nanostructures by solving Schrodinger equation assuming the barriers have an infinite confining potential. The "effective mass" solutions of the Schrödinger equation for electrons confined in a quantum dot or NCs, quantum wire and quantum well are,

Quantum dot or Nanocrystals:

$$E_{n,m,l} = \frac{\pi^2\hbar^2}{2m^*}\left(\frac{n^2}{L_z^2}+\frac{m^2}{L_y^2}+\frac{l^2}{L_x^2}\right), \psi = \phi(z)\phi(y)\phi(x) \text{ --------------------------} \quad (2)$$

Quantum wire:

$$E_{n,m}(k_x) = \frac{\pi^2\hbar^2}{2m^*}\left(\frac{n^2}{L_z^2}+\frac{m^2}{L_y^2}\right)+\frac{\hbar^2 k_x^2}{2m^*}, \psi = \phi(z)\phi(y)\exp(ik_x x) \text{ ----------------} \quad (3)$$

Quantum well:

$$E_n(k_x k_y) = \frac{\pi^2\hbar^2 n^2}{2m^* L_z^2}+\frac{\hbar^2}{2m^*}\left(k_x^2+k_y^2\right), \psi = \phi(z)\exp\left(ik_x x+ik_y y\right) \text{ --------------} \quad (4)$$

where *n, m, l* = 1, 2 … the quantum confinement numbers, L_x, L_y and L_z are the confining dimensions, $\exp\left(ik_x x+ik_y y\right)$ is the wave function describing the electronic motion in *x* and *y* direction, similar to free electron wave functions. A brief reference to quantum wells and its properties follows in the next section.

1.2. Quantum well structures and its properties

A quantum well is a particular kind of heterostructure in which one thin "well" layer is surrounded by two "barrier" layers. Both electrons and holes see lower energy in the "well" layer, hence the name by analogy with a "potential well". This layer, in which both electrons and holes are confined, is so thin (typically about 100 Å or about 40 atomic layers) that we cannot neglect the fact that the electron and hole are both waves. In fact, the allowed states in this structure correspond to standing waves in the direction perpendicular to the layers. Because

only particular waves are standing waves, the system is quantized, hence the name "quantum well"(Scully et al. 1999).

One-dimensional quantum wells are formed through epitaxial growth of alternating layers of semiconductor materials with different band gaps. A single quantum well is formed from one semiconductor sandwiched between two layers of a second semiconductor having a larger band gap. The centre layer with the smaller band gap semiconductor forms the QW, while the two layers sandwiching the centre layer create the potential barriers as shown in Fig. 1.3. Two potential wells are actually formed in the QW structure; one well is for conduction-band electrons, the other for valence-band holes. The well depth for electrons is the difference (*i.e.* the offset) between the conduction-band edges of the well and barrier semiconductors, while the well depth for holes is the corresponding valence-band offset. Multiple quantum well structures consist of a series of QWs (*i.e.* a series of alternating layers of wells and barriers). If the barrier thickness between adjacent wells is sufficient to prevent significant electronic coupling between the wells, then each well is electronically isolated; this type of structure is termed as *multiple quantum well*. Quantum wells are thin layered semiconductor structures in which we can observe and control many quantum mechanical effects. They derive most of their special properties from the quantum confinement of charge carriers (electrons and "holes") in thin layers (e.g 40 atomic layers thick) of one semiconductor "well" material sandwiched between other semiconductor "barrier" layers. We can understand the basic properties of a quantum well through the simple "particle in a box" model. Here we consider Schrödinger's equation (Neuhasuer and Baer 1989) in one dimension for the particle of interest (e.g., electron or hole),

$$\frac{\hbar^2}{2m}\frac{d^2\phi_n}{d_Z{}^2}+V(z)\phi_n=E_n\phi_n \text{ ----------------------- } \quad (5)$$

where V(z) is the structural potential (i.e., the "quantum well" potential) seen by the particle along the direction of interest (z), m is the particle's (effective) mass, and E_n and ϕ_n are the Eigen energy and Eigen function associated with the nth solution to

Fig. 1.3: *One-dimensionally confined quantum well created by a thin small-band gap semiconductor layer sandwiched between two larger band gap semiconductor layers.* E_g^{Well} *is the band gap of the well material and* $E_g^{barrier}$ *that of the barrier material.*

Fig. 1.4: *Infinite quantum well and associated wave functions.*

the equation. The simplest case is shown in Fig. 1.4. In this "infinite well" case, we presume for simplicity that the barriers on either side of the quantum well are infinitely high. Then the wave function must be zero at the walls of the quantum well. The solution is then particularly simple:

$$E_n = \frac{\pi^2 \hbar^2 n^2}{2m^* L_z^2} \quad n = 1, 2..... \quad \phi_n = A \sin(\frac{n\pi z}{L_Z}) \quad \text{---------} \qquad (6)$$

The energy levels (or "confinement energies") are quadratically spaced, and the wave functions are sine waves. In this formula, the energy is referred to the energy of the bottom of the well. Note that the first allowed energy (corresponding to n=1) is above the bottom of the well. We see that the energy level spacing becomes large for narrow wells (small L_z) and small effective mass m. The actual energy of the first allowed electron energy level in a typical 100 Å GaAs quantum well is about 40 meV, which is close to the value that would be calculated by this simple formula. This scale of energy is easily seen, even at room temperature. The solution of the problem of an actual quantum well with finite height of barriers is a straightforward mathematical exercise. It does, however, require that we choose boundary conditions to match the solutions in the well and the barriers. One boundary condition is obvious, which is that the wave function must be continuous.

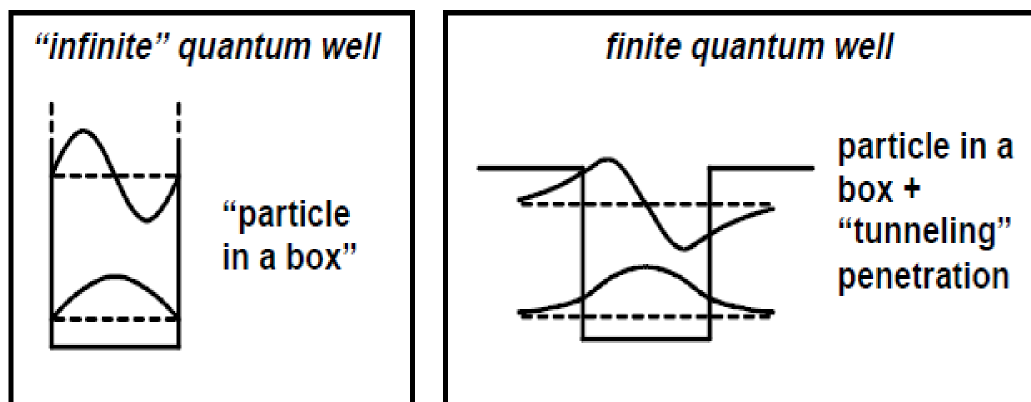

Fig. 1.5: *Comparison of "infinite" quantum well and “finite" quantum well behaviour.*

Since the Schrödinger equation is a second order equation, we need a second boundary condition, and it is not actually obvious what it should be. Fig. 1.5 illustrates the differences between the idealized "infinite" quantum well, the actual "finite" well.

In contrast to bulk semiconductors, excitonic effects are very clear in quantum wells at room temperature, and have a significant influence on device performance. The simplest model for absorption between the valence and conduction bands in a bulk semiconductor is to say that we can raise an electron from the valence band to a state of essentially the same momentum in the conduction band (a "vertical" transition) by absorbing a photon. The state in the conduction band has to have essentially the same momentum because the photon has essentially no momentum on the scale usually of interest in semiconductors. In this simple model, we also presume that all such transitions have identical strength, although they will have different energies corresponding to the different energies for such vertical transitions. The optical absorption spectrum therefore has a form that follows directly from the density of states in energy, and in bulk semiconductors the result is an absorption edge that rises as the square root of energy, as shown in Fig. 1.6.(Reed et al. 1988).

In a quantum well, the electrons and holes are still free to move in the directions parallel to the layers; hence, we do not really have discrete energy states for electrons and holes in quantum wells; we have instead "sub-bands" that start at the energies calculated for the confined states. The electron in a given confined state can in addition have any amount of kinetic energy for its in-plane motion in the quantum well, and so can have any energy greater than or equal to the simple confined-state energy for that sub-band. The density of states for motion in the plane of the quantum well layers turns out to be constant with energy, so the density of states for a given sub-band really is a "step" that starts at the appropriate confinement energy.

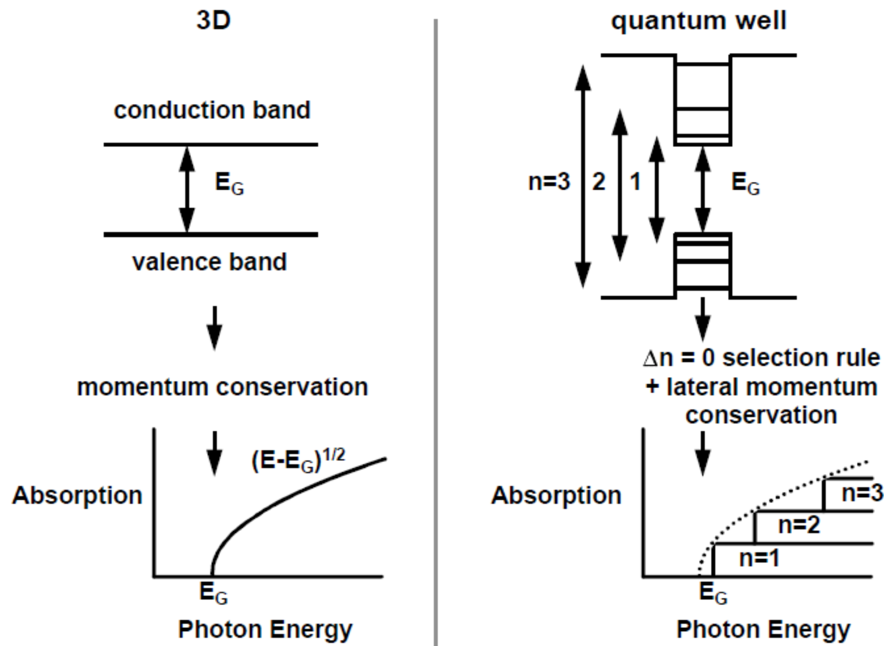

Fig. 1.6: *Optical absorption in bulk (i.e., 3D) semiconductors and in quantum wells.*

Optical transitions must still conserve momentum in this direction and just as for bulk semiconductors; the optical absorption must still therefore follow the density of states. Hence, in this simple model, the optical absorption in a quantum well is a series of steps, with one step for each quantum number, n. It is easily shown, from the known densities of states, that the corners of the steps "touch" the square root bulk absorption curve (when that curve is scaled to the thickness of this infinite quantum well). Thus, as we imagine increasing the quantum well thickness, we will make a smooth transition to the bulk behaviour, with the steps becoming increasingly close until they merge into the continuous absorption edge of the bulk material. For example, room temperature absorption spectrum of a GaAs/ $Al_{0.28}Ga_{0.72}As$ MQW structure containing 40 periods with 7.6 GaAs quantum well is shown in Fig. 1.7(Han et al. 1998). The spectrum of GaAs at the same temperature is shown for comparison. We see from Fig. 1.7 that the quantum well absorption is indeed a series of steps, and simple calculations based on the particle-in-a-box models will correctly give the approximate positions of the steps.

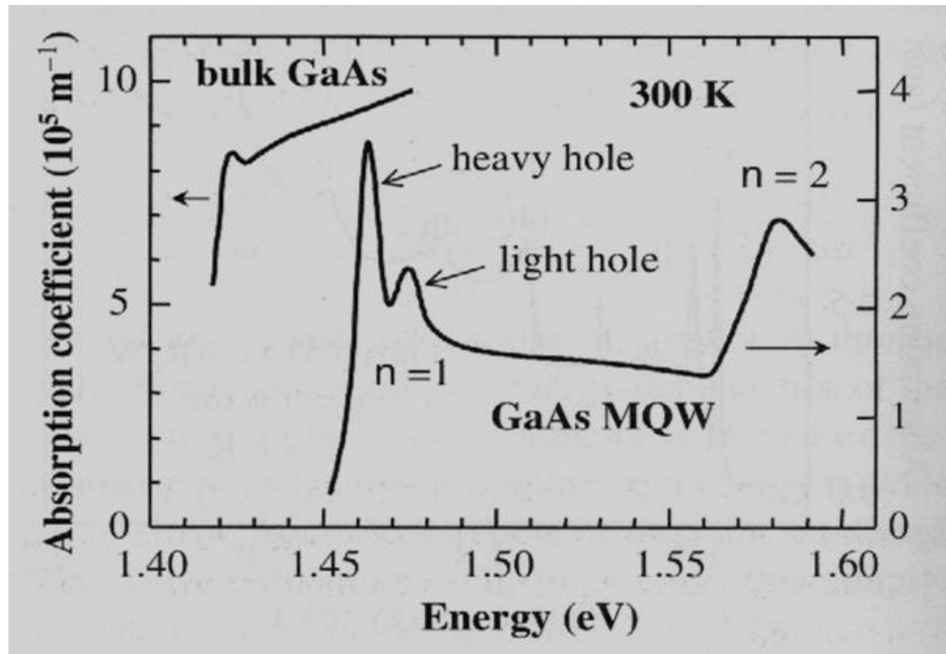

Fig. 1.7: *Room temperature absorption spectrum of GaAs/ $Al_{0.28}Ga_{0.72}As$ MQW structure (Courtesy:(Han et al. 1998).*

Detailed analysis reveals that the binding energies of the quantum well excitons are about 10 meV, higher than the value of 4.2 meV in bulk GaAs. The enhancement is a consequence of the quantum confinement of the electrons and holes in the QW. The excitons are still stable at room temperature in the QW. The bulk sample merely shows a weak shoulder at band edge, but the MQW shows strong peaks for both the heavy and the light hole excitons. The lifting of the degeneracy originates from the different effective masses of the heavy and light holes and the lower symmetry of the QW sample.

1.3. Quantum wells in optoelectronic devices

Semiconductor quantum wells are excellent examples of quantum mechanics in action. The reduced dimensionality has led to major advances in both the understanding of 2-D physics and the applied science of optoelectronics. In this section the applications of QW for optoelectronic devices is discussed. The discussion will also show how these optoelectronic devices incorporated with QW ultimately attain the best of both electronic and optical worlds. A new physical

mechanism in such thin layered QW structures make real devices with very attractive performance characteristics and impressive yields. The special properties of very thin layers come from the relatively simple quantum mechanical problem of confining particles in a box or well. Here we describe a few kinds of optoelectronic devices incorporated with QW structure namely LED and laser diode, quantum cascade laser, Detectors such as inter sub-band detector and solar cells.

1.3.1. Light emitting diodes and Laser diodes

Quantum wells have found widespread use in LED and laser diode applications for a number of years now (Vinokurov et al. 2010). There are three main reasons for this. Firstly, the ability to control the quantum-confinement energy provides an extra degree of freedom to engineer the emission wavelength. Secondly, the change of the density of states and the enhancement of the electron–hole overlap leads to superior performance. Finally, the ability to grow strained layers of high optical quality greatly increases the variety of material combinations that can be employed, thus providing much greater flexibility in the design of the active regions. Much of the early work concentrated on lattice matched combinations such as GaAs/AlGaAs (Tomioka et al. 2010, Vinokurov et al. 2010). GaAs/AlGaAs QW lasers operating around 800 nm has now become industry-standard for applications in laser printers and compact discs. Furthermore, the development of high power arrays has opened up new applications for pumping solid-state lasers such as Nd: YAG. Other types of lattice-matched combinations can be used to shift the wavelength into the visible spectral region and also further into the infrared. QWs based on the quaternary alloy $(Al_yGa_{1-y})_x In_{1-x}P$, are used for red-emitting laser pointers while $Ga_{0.47} In_{0.53} As$ QWs and its variants incorporating Al are used for the important telecommunication wavelengths of 1300 nm and 1550 nm (Akimoto et al. 2005). A major application of quantum wells is in *vertical cavity surface-emitting lasers* (Grabherr et al. 1997). Fig.1.8 gives a schematic diagram of a typical GaAs-based VCSEL. The device contains an active QW region inserted between two distributed Bragg reflector mirrors consisting of AlGaAs quarter wave stacks

made of alternating high and low refractive index layers. The structure is grown on an n-type GaAs substrate, and the mirrors are appropriately doped with p-type to form a p–n junction. Electrons and holes are injected into the active region under forward bias, where they are captured by the QWs and produce gain at the lasing wavelength λ. The quantum wells are contained within a transparent layer of thickness $\lambda / 2n_0$, where n_0 is the average refractive index of the active region.

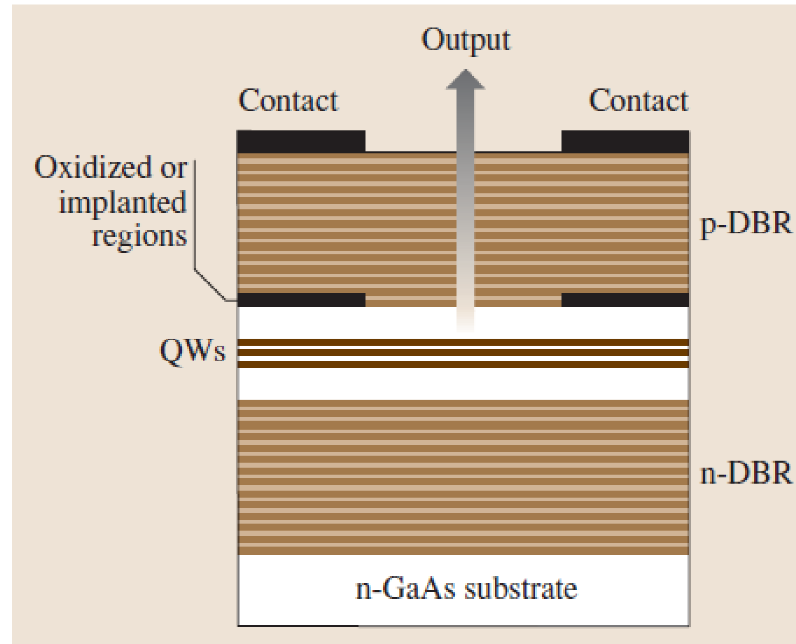

Fig. 1.8: *Schematic diagram of a VCSEL. The QWs that comprise the gain medium are placed at the centre of the cavity formed between two distributed Bragg reflector mirrors. Oxidised or proton-implanted regions provide the lateral confinement for both the current and the optical mode.*

The light at the design wavelength is reflected back and forth through the gain medium and added up constructively, forming a laser resonator. Oxidised or proton-implanted regions provide lateral confinement of both the current and the optical mode. The conventional VCSEL structures grown on GaAs substrates operate in the wavelength range 700 –1100 nm (Grabherr et al. 1997). Some of these structures are lattice matched, but others notably the longer wavelength devices which incorporate strained InGaAs quantum wells are not. Much work is currently focussed on extending the range of operation to the telecommunication

wavelengths of 1300 nm and 1550 nm. Resonator structures such as the VCSEL shown in Fig. 1.8 can be operated below threshold as resonant cavity LEDs. The presence of the cavity reduces the emission line width and hence increases the intensity at the peak wavelength. Furthermore, the narrower line width leads to an increase in the bandwidth of the fibre communication system due to the reduced chromatic dispersion.

1.3.2. Quantum Cascade Lasers

The principles of infrared emission by inter sub-band transitions that electrons must first be injected into an upper confined electron level (Liu et al. 2003). Radiative transitions to lower confined states with different parities can then occur. ISB emission is usually very weak, as the radiative transitions have to compete with very rapid non radiative decay by phonon emission. However, when the electron density in the upper level is large enough, population inversion can occur, giving rapid stimulated emission and subsequent laser operation. This is the operating concept of the *quantum cascade laser* first demonstrated in 1994 (Faist et al. 1994). The laser operated at 4.2μm at temperatures up to 90K. Although the threshold current for the original device was high, progress in the field had been very rapid. The quantum well structures used in QC lasers are very complicated, and often contain hundreds of different layers. Fig. 1.9 illustrates a relatively simple design based on lattice-matched $In_{0.47}Ga_{0.53}As/Al_{0.48}In_{0.52}$. As quantum wells grown on an InP substrate (Yang et al. 2013). The diagram shows two active regions and the miniband injector region that separates them. A typical operational laser might contain 20-30 such repeat units. The population inversion is achieved by resonant tunnelling between the $n = 1$ ground state of one active region and the $n = 3$ upper laser level of the next one. The basic principles of this process were enunciated as early as 1971, but it took more than 20 years to demonstrate the ideas in the laboratory. The active regions contain asymmetric coupled quantum wells, and the laser transition takes place between the $n = 3$ and $n = 2$ states of the coupled system.

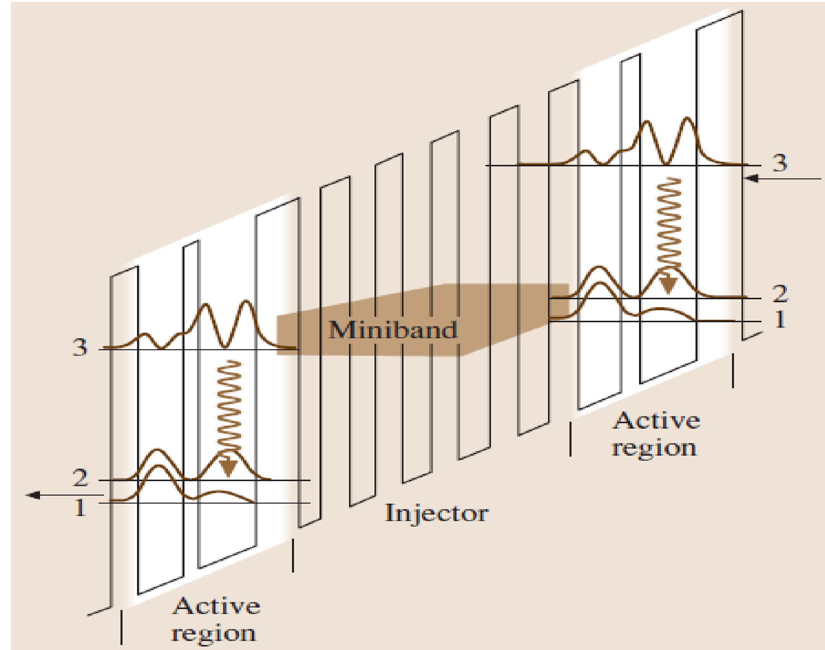

Fig. 1.9: *Conduction band diagram for two active regions of an InGaAs/AlInAs quantum cascade laser, together with the intermediate mini-band injector region. The levels in each active region are labelled according to their quantum number n, and the corresponding wave function probability densities are indicated. Laser transitions are indicated by the wavy arrows, while electron tunnelling processes are indicated by the straight arrows.*

The separation of the $n = 2$ and $n = 1$ levels is carefully designed to coincide with the LO-phonon energy, so that very rapid relaxation to the ground state occurs and the system behaves as a four-level laser. This latter point is crucial, since the lifetime of the upper laser level is very short (typically ≈ 1 ps), and population inversion is only possible when the lifetime of the lower laser level is shorter than that of the upper one. The lasing wavelength can be varied by detailed design of the coupled QW active region. A very interesting development has been the demonstration of a QC laser operating in the far-infrared spectral region at 87μm (Yang et al. 2013). Previous work in this spectral region had been hampered by high losses due to free-carrier absorption and the difficulties involved in designing the optical waveguides. The device operated up to 50K and delivered 2mW. These

long-wavelength devices are required for applications in the THz frequency range that bridges between long wavelength optics and high frequency electronics.

1.3.3. Quantum well Solar Cells

Photo detectors for the visible and near-infrared spectral regions are generally made from bulk silicon or III-V alloys such as GaInAs. Since these devices work very well, the main application for QW photo detectors is in the infrared spectral region and for especially demanding applications such as ISB photo detector and solar cells.

The power generated by a solar cell is determined by the product of the photocurrent and the voltage across the diode. In conventional solar cells, both of these parameters are determined by the band gap of the semiconductors used. Large photocurrents are favoured by narrow gap materials, because semiconductors only absorb photons with energies greater than the band gap, and narrow gap materials therefore absorb a larger fraction of the solar spectrum (López et al. 2011). However, the largest open circuit voltage that can be generated in a p-n device is the built in voltage which increases with the band gap of the semiconductor. Quantum well devices can give better performance than their bulk counterparts because they permit separate optimisation of the current and voltage generating factors (Anderson 1995). This is because the built in voltage is primarily determined by the band gap of the barrier regions, whereas the absorption edge is determined by the band gap of the quantum wells. The quantum well solar cell is composed of a p-i-n diode with quantum wells located in the intrinsic region of the device. A schematic representation of the cell is shown in Fig. 1.10(a), while Fig. 1.10(b) shows the associated band diagram together with the main carrier photo generation and recombination paths in the barrier and QW layers.

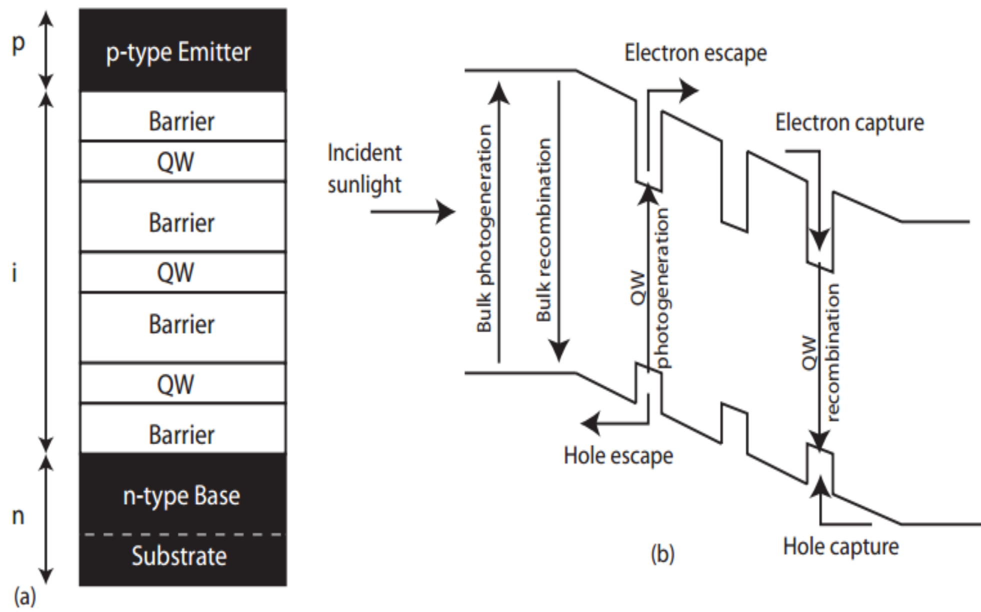

Fig. 1.10: *(a) Quantum well p-i-n layer structure. (b) Band diagram for the quantum well p-i-n solar cell showing the photogeneration and recombination processes, together with the carrier capture and escape routes. (courtesy: (Ekins-Daukes et al. 2013)).*

The light absorbed in the quantum wells results in the generation of electron–hole pairs in the confined well. Before these electrons and holes can contribute to the photocurrent, the carriers must escape from the quantum well through a combination of thermal and tunnelling processes shown schematically in Fig 1.10 together with the corresponding carrier capture process. The carrier escape is efficient providing that there is sufficient thermal energy and the transverse electric field is sufficiently strong (Ekins-Daukes et al. 2013). In many quantum well solar cells at room temperature, both the carrier capture and escape processes proceed faster than competing recombination processes, resulting in an equilibration within the conduction and valance bands between carriers in the barrier and QW layers. From a practical standpoint, this means that all photogenerated carriers in shallow quantum well can be assumed to escape and contribute towards the photocurrent (Araujo et al. 1999).

1.3.4. Inter-Sub-Band photo Detectors

Infrared detectors are required for applications in defence, night vision, astronomy, thermal mapping, gas sensing, and pollution monitoring. *Quantum well inter-sub-band photodetectors* are designed so that the energy separation of the confined levels is matched to the chosen wavelength (Schneider et al. 1991). A major advantage of QWIPs over the conventional approach employing narrow band gap semiconductors is the use of mature GaAs based technologies. Furthermore, the detection efficiency should in principle be high due to the large oscillator strength that follows from the parallel curvature of the in plane dispersions for states within the same bands. However, technical challenges arise from the requirement that the electric field of the light must be polarised along the growth (z) direction. Various approaches have been taken for optimum light coupling, such as using bevelled edges, gratings or random reflectors. Despite their promising characteristics, QWIPs have yet to be commercialised. The main issue is the high dark current at higher operating temperatures. The dark current is governed by the thermionic emission of ground-state electrons directly out of the QW above 45K. Overcoming such technical difficulties has made possible for the demonstration of long wavelength large format focal plane array cameras based on ISB transitions.

1.4. Problem statement and Motivation

Quantum confinement effects on PbSe have been investigated by several authors using chemical method of preparation as a convenient method (Choi et al. 2009, Wise 2000). Reported works on PbSe NCs mainly concern with size reduction results in strong quantum confinement confirmed only through optical properties. On PbSe NCs, only preliminary work has been done and in fact, its electronic coupling between the NCs itself has not been resolved yet. Drawbacks of the chemical methods on the formation of PbSe NCs are temperature instability, less absorption yield and sparse NCs which result in reduction of electronic coupling between the NCs, as discussed in the introduction part. These factors are crucial for device manufacturing, and physical methods are therefore preferred.

Quantum confinement of semiconductor materials using physical methods can be realised by MQW, superlattice formation and multilayer like composite structure (Nesheva and Hofmeister 2000, Park et al. 2003). There are very few reports available based on PbSe MQW, and most of them are dealing with IR detectors and optical windows rather than quantum dot solar cells (Ishida et al. 1987). Since, the quantum size effect of PbSe using chemical method of preparation have been understood fairly well, it is of our interest to investigate the quantum size effect by physical method of preparation using multiple quantum well approach with comparatively wide band gap ZnSe barrier layers.

Even though PbSe NCs are identified as a promising material for MEG, it is strongly active in near-IR region rather than visible region. Recent solar cells research focuses on not only carrier multiplication and fast hot electron transport, but also on utilizing the full solar spectrum (UV-NIR). For example, polymer-ZnSe nanocrystal hybrid photovoltaic solar cells show NIR absorption together with improved efficiency upon insertion of PbSe NCs layers (Yun et al. 2009). In fact, the nature of ZnSe will absorb the energy in visible region and quantum confined 2D PbSe QW layers will give complementary NIR absorption to ZnSe towards full solar spectrum utilization. Apart from shift in optical band gap due to quantum size effect, PbSe will generate multiple excitons from single absorbed photon (Schaller et al. 2006, Choi et al. 2009).

For preparation of multilayers with good stability and periodicity, molecular beam epitaxy or metal-organic chemical vapour deposition are most frequently applied (Lee et al. 1999). However, both techniques are quite expensive and, in MOCVD normally use dangerous gases. Beside this, high quality crystalline ZnSe, GaAs or sapphire substrates are necessary for the epitaxial growth. Therefore a considerable research activity has been addressed for the preparation of low-dimensional structures by non-epitaxial film growth and application of less expensive vapour deposition (Nesheva et al. 2012, Allen, Shih and Potter 2010).

1.5. Objective of the work

The objective of the work is to investigate the quantum confinement effect in PbSe/ZnSe MQW structures by simple thermal evaporation technique with well-defined periodic structure as a function of quantum well thickness, quantum well period and impact of annealing.

In order to achieve the objective, the following work elements have been set.

- Preparation of PbSe/ZnSe MQW structure with a QW thickness ranges from 2.5 to 10 nm with the interval of 2.5 nm. The period of QW structure was varied as 5, 10 and 20
- In order to investigate the size reduction of 2D layers of PbSe at the interfaces with elongated surface morphology, mild thermal treatment was applied to "'break-up'" the less thermal coefficient material of PbSe
- Studying the quantum size effect by means of blue shift and energy level splitting
- The research findings of the work came from the characterizations using HRXRD, cross sectional TEM, optical absorption spectra, photoluminescence and Raman scattering.